High Population of Individualized SWCNTs through the Adsorption of Water-Soluble Perylenes

ARTICLE *in* JOURNAL OF THE AMERICAN CHEMICAL SOCIETY · FEBRUARY 2009

Impact Factor: 12.11 · DOI: 10.1021/ja805660b · Source: PubMed

5 AUTHORS, INCLUDING:

Claudia Backes
Universität Heidelberg
42 PUBLICATIONS **811** CITATIONS
SEE PROFILE

Cordula D. Wessendorf
Zentrum für Sonnenenergie und Wassersto…
24 PUBLICATIONS **734** CITATIONS
SEE PROFILE

J|A|C|S ARTICLES

Published on Web 01/26/2009

High Population of Individualized SWCNTs through the Adsorption of Water-Soluble Perylenes

Claudia Backes,[†] Cordula D. Schmidt,[†] Frank Hauke,[†] Christoph Böttcher,[‡] and Andreas Hirsch*[,†]

Department of Chemistry and Pharmacy & Central Institute of Advanced Materials and Processes (ZMP), University of Erlangen-Nürnberg, Henkestrasse 42, 91054 Erlangen, Germany, and Forschungszentrum für Elektronenmikroskopie, Institut für Chemie and Biochemie, Freie Universität Berlin, Fabeckstrasse 36a, 14195 Berlin, Germany

Received July 31, 2008; E-mail: andreas.hirsch@chemie.uni-erlangen.de

Abstract: The aqueous dispersion of SWCNTs in the presence of the water-soluble perylene derivatives **1**−**3** is reported. Significantly, even very low concentrations of the perylenes such as 0.01 wt% of the amphiphilic derivative **3**, cause an efficient dissolution of the SWCNTs in water accompanied by a very pronounced individualization. The individualization of SWCNTs in water after ultrasonication in the presence of water-soluble aromatic perylenes was investigated in detail by absorption, emission, and Raman spectroscopy as well as by AFM and cryo-TEM. These studies also revealed that the individualization of the SWCNTs caused by the adsorption of **3** is much more effective than that induced by SDBS, which is the most frequently used surfactant for SWCNT dispersion in water. The $\pi-\pi$-stacking interaction and the electronic interaction between the perylene unit and the nanotube surface is reflected, for example, by the distinct absorption and emission features in the UV/vis/nIR, which differ significantly from those observed for SWNTs dispersed in the presence of SDBS and by the quenching of the perylene fluorescence of **3** when being in contact with the tubes.

Introduction

The field of carbon nanotube research has exceptionally blossomed within the past decade. The scientific interest is driven by the remarkable potential of this extraordinary new carbon allotrope. Their unique one-dimensional structure and therefore their outstanding electronic, thermal, and mechanical properties are unrivaled by any other substance class.[1−3] However, all proposed applications[1−6] have so far been limited by their virtual insolubility in aqueous and organic solvents,[7,8] as well as the diversity of tube diameters, chiral angles, and aggregation. Therefore, it is desirable to find ways to disperse SWCNTs in various media[9,10] on the one hand and separate SWCNTs of different diameter and chiral angle on the other hand.[11,12] In order to overcome the high van der Waals attraction of 0.5 eV/μm between the individual SWCNTs[13,14] in a carbon nanotube bundle[15] it was quickly recognized that the chemical functionalization can be one keystone in solubilizing SWCNTs.[16−20] Although chemical functionalization can drastically enhance the solubility of SWCNTs in various solvents, it also alters the intrinsic physical properties of the carbon nanotubes because of a modification of the sp^2-carbon framework. Noncovalent functionalization by polymer wrapping,[21,22] interaction with

[†] University of Erlangen-Nürnberg.
[‡] Freie Universität Berlin.

(1) Dresselhaus, M. S.; Dresselhaus, G.; Avouris, P. *Carbon Nanotubes: Synthesis, Structure, Properties, and Applications*; Springer: Berlin, 2001.
(2) Ouyang, M.; Huang, J.-L.; Lieber, C. M. *Acc. Chem. Res.* **2002**, *35*, 1018–1025.
(3) Rotkin, S. V.; Subramoney, S. *Applied Physics of Carbon Nanotubes: Fundamentals of Theory, Optics and Transport Devices*; Springer: Berlin, 2005.
(4) Baughman, R. H.; Zakhidov, A. A.; de Heer, W. A. *Science* **2002**, *297*, 787–792.
(5) Avouris, P. *Acc. Chem. Res.* **2002**, *35*, 1026–1034.
(6) Tanaka, K.; Yamabe, T.; Fukui, K. *The Science and Technology of Carbon Nanotubes*; Elsevier: Oxford, 1999.
(7) Bahr, J. L.; Mickelson, E. T.; Bronikowski, M. J.; Smalley, R. E.; Tour, J. M. *Chem. Commun.* **2001**, 193–194.
(8) Ausman, K. D.; Piner, R.; Lourie, O.; Ruoff, R. S.; Korobov, M. *J. Phys. Chem. B* **2000**, *104*, 8911–8915.
(9) Furtado, C. A.; Kim, U. J.; Gutierrez, H. R.; Pan, L.; Dickey, E. C.; Eklund, P. C. *J. Am. Chem. Soc.* **2004**, *126*, 6095–6105.
(10) Kim, D. S.; Nepal, D.; Geckeler, K. E. *Small* **2005**, *1*, 1117–1124.
(11) Banerjee, S.; Hemraj-Benny, T.; Wong, S. S. *J. Nanosci. Nanotechnol.* **2005**, *5*, 841–855.
(12) Krupke, R.; Hennrich, F.; Lohneysen Hilbert, v.; Kappes, M. *Science* **2003**, *301*, 344–7.
(13) Girifalco, L. A.; Hodak, M.; Lee, R. S. *Phys. Rev. B* **2000**, *62*, 13104–13110.
(14) Nuriel, S.; Liu, L.; Barber, A. H.; Wagner, H. D. *Chem. Phys. Lett.* **2005**, *404*, 263–266.
(15) Thess, A.; Lee, R.; Nikolaev, P.; Dai, H.; Petit, P.; Robert, J.; Xu, C.; Lee, Y. H.; Kim, S. G.; Rinzler, A. G.; Colbert, D. T.; Scuseria, G. E.; Tománek, D.; Fischer, J. E.; Smalley, R. E. *Science* **1996**, *273*, 483–487.
(16) Hirsch, A. *Angew. Chem., Int. Ed.* **2002**, *41*, 1853–1859.
(17) Banerjee, S.; Kahn Michael, G. C.; Wong, S. S. *Chem. Eur. J.* **2003**, *9*, 1898–908.
(18) Banerjee, S.; Hemraj-Benny, T.; Wong, S. S. *Adv. Mater.* **2005**, *17*, 17–29.
(19) Hirsch, A.; Vostrowsky, O. *Top. Curr. Chem.* **2005**, *245*, 193–237.
(20) Tasis, D.; Tagmatarchis, N.; Bianco, A.; Prato, M. *Chem. Rev.* **2006**, *106*, 1105–1136.
(21) Star, A.; Liu, Y.; Grant, K.; Ridvan, L.; Stoddart, J. F.; Steuerman, D. W.; Diehl, M. R.; Boukai, A.; Heath, J. R. *Macromolecules* **2003**, *36*, 553–560.
(22) Hwang, J.-Y.; Nish, A.; Doig, J.; Douven, S.; Chen, C.-W.; Chen, L.-C.; Nicholas, R. J. *J. Am. Chem. Soc.* **2008**, *130*, 3543–3553.

 10.1021/ja805660b CCC: $40.75

biomolecules such as DNA[23,24] or peptides[25] and the adsorption of ionic or nonionic surfactants[26−36] has emerged as the most promising tool for SWCNT solubilizition in combination with the preservation of the intrinsic electronical and mechanical properties. Moreover, Arnold et al. have recently reported on the separation of specific chiralities of SWCNTs with the aid of surfactants in density gradient ultracentrifugation.[37] Further reports have underlined the importance of the surfactant used: by varying the surfactant or adding a cosurfactant, separation has found to occur via either diameter or electronic type of the nanotube.[38−40] According to Wenseleers et al.,[27] efficient solubilization of SWCNTs is provided by surfactants forming very stable micelle structures around the nanotubes. Furthermore, the formation of a large solvation shell due to long and disordered polar tails is favorable, especially if the polar tail is charged, as nanotube aggregation is then further prevented by Coulombic repulsion between the surfactant-coated SWCNTs. In our opinion, a molecule containing a hydrophilic dendritic structure and simultaneously bearing an apolar polyaromatic subunit ensuring a strong interaction with the SWCNTs would perfectly fulfill these structural requirements for an ideal SWCNT surfactant. Therefore, our interest has focused on the use of water-soluble Newkome-dendronized perylenetetracarboxydiimides[41] as an aromatic amphiphile for the dispersion of SWCNTs in aqueous media. Similar to polycyclic aromatic ammonium amphiphiles which have been reported to solubilize carbon nanotubes,[42] the structure consists of a polycyclic aromatic moiety adsorbing on the nanotube surface via $\pi-\pi$ stacking and a solvophilic moiety to aid dissolution in dipolar solvents such as water. Apart from the aspects concerning dispersion and separation mentioned above, the perylene bisimide used in this work might be of interest for integrating SWCNTs in nanohybrids, as previously described by Guldi et al. for other polycyclic aromatic hydrocarbon moieties.[43−45] In this regard the electronic communication such as photoinduced electron- or energy-transfer between the tubes and the adsorbed chromophores is of particular interest for the development of new photovoltaic devices.

Experimental Details

General. SWCNTs were obtained from Carbon Nanotechnologies Inc. (Purified HiPco-Single-Wall Carbon Nanotubes, batch number: P0343) and used as received. Chemicals and solvents were purchased from Acros (Geel, Belgium) and also used as received. The synthesis of the perylene bisimide derivative was performed according to the procedure described elsewhere.[41]

Raman spectra of each sample were measured from the solid (buckypaper) and in solution by a Horiba Jobin Yvon LabRAM Aramis Raman Spectrometer ($\lambda_{exc} = 532$, 633, and 785 nm). All spectra have been normalized to the G-band. Fluorescence spectra of the nanotubes in an aqueous solution of SDBS (1 wt%) and buffered aqueous solutions of perylene **3** (Per3) were recorded with a NS1NanoSpectralyzer ($\lambda_{exc} = 660$ and 785 nm) from Applied NanoFluorescence, LLC. Unless otherwise noted, the spectra were normalized to the maximum at 1160 nm (660 nm excitation) and 1140 nm (785 nm excitation). For the acquisition of the UV/vis/nIR absorption spectra, a Shimadzu UV3102-PC instrument was used. Unless otherwise noted, both fluorescence and UV/vis/nIR spectra were measured after sonication (30 min, 80 W, 45 kHz) from the supernatant after centrifugation with a 4K15 Sigma centrifuge (15 000 rpm, 30 min, 15 °C). Fluorescence of the Per3 was measured with a Shimadzu RF-5301 PC spectrometer with $\lambda_{exc} = 500$ nm and a slid width of 5 nm. AFM images were recorded on a Solver Pro (Scanning Probe Microscope), NT-MDT Co. The carbon nanotube material was spread on oxidized silicon wafers by spin coating.

Cryo-TEM. Droplets of the sample (5 μL) were applied to perforated (1 μm hole diameter) carbon film covered 200 mesh grids (R1/4 batch of Quantifoil Micro Tools GmbH, Jena, Germany), which had been hydrophilized before use by 60 s plasma treatment at 8 W in a BALTEC MED 020 device. The supernatant fluid was removed with a filterpaper until an ultrathin layer of the sample solution was obtained spanning the holes of the carbon film. The samples were immediately vitrified by propelling the grids into liquid ethane at its freezing point (90 K) operating a guillotine-like plunging device. The vitrified samples were subsequently transferred under liquid nitrogen into a Tecnai F20 FEG transmission electron microscope (FEI Company, Hillsboro, Oregon) using the Gatan (Gatan Inc., Pleasanton, California) cryoholder and cryostage (Model 626). Microscopy was carried out at 94 K sample temperature using the microscopes low dose protocol at a calibrated primary magnification of 62 000× and an accelerating voltage of 160 kV (FEG- illumination). Images were recorded with an Eagle 2k CCD camera at full size read-out area and binning 1×. The defocus was chosen in all cases to be 2 μm.

Preparation of the SWCNT−Per Composites. To the appropriate amount of of HiPco SWCNTs, buffered solutions (phosphate buffer, pH = 7.0) of **1** (*N*,*N*′-bis(5-carboxy{4-[(2-carbonyl)ethyl]-4-aminoheptane}pentyl)-perylene-3,4,9,10-tetracarboxybisimide), **2** (*N*,*N*′-bis(5-

(23) Nakashima, N.; Okuzono, S.; Murakami, H.; Nakai, T.; Yoshikawa, K. *Chem. Lett.* **2003**, *32*, 456–457.
(24) Zheng, M.; Jagota, A.; Semke, E. D.; Diner, B. A.; McLean, R. S.; Lustig, S. R.; Richardson, R. E.; Tassi, N. G. *Nat. Mater.* **2003**, *2*, 338–342.
(25) Witus, L. S.; Rocha, J.-D. R.; Yuwono, V. M.; Paramonov, S. E.; Weisman, R. B.; Hartgerink, J. D. *J. Mater. Chem.* **2007**, *17*, 1909–1915.
(26) O'Connell, M. J.; Bachilo, S. M.; Huffman, C. B.; Moore, V. C.; Strano, M. S.; Haroz, E. H.; Rialon, K. L.; Boul, P. J.; Noon, W. H.; Kittrell, C.; Ma, J.; Hauge, R. H.; Weisman, R. B.; Smalley, R. E. *Science* **2002**, *297*, 593–596.
(27) Wenseleers, W.; Vlasov, I. I.; Goovaerts, E.; Obraztsova, E. D.; Lobach, A. S.; Bouwen, A. *Adv. Funct. Mater.* **2004**, *14*, 1105–1112.
(28) Ishibashi, A.; Nakashima, N. *Chem. Eur. J.* **2006**, *12*, 7595–7602.
(29) Ke, P. C. *Phys. Chem. Chem. Phys.* **2007**, *9*, 439–447.
(30) Matarredona, O.; Rhoads, H.; Li, Z.; Harwell, J. H.; Balzano, L.; Resasco, D. E. *J. Phys. Chem. B* **2003**, *107*, 13357–13367.
(31) Islam, M. F.; Rojas, E.; Bergey, D. M.; Johnson, A. T.; Yodh, A. G. *Nano Lett.* **2003**, *3*, 269–273.
(32) Moore, V. C.; Strano, M. S.; Haroz, E. H.; Hauge, R. H.; Smalley, R. E.; Schmidt, J.; Talmon, Y. *Nano Lett.* **2003**, *3*, 1379–1382.
(33) Okazaki, T.; Saito, T.; Matsuura, K.; Ohshima, S.; Yumura, M.; Iijima, S. *Nano Lett.* **2005**, *5*, 2618–2623.
(34) Bergin, S. D.; Nicolosi, V.; Cathcart, H.; Lotya, M.; Rickard, D.; Sun, Z.; Blau, W. J.; Coleman, J. N. *J. Phys. Chem. C* **2008**, *112*, 972–977.
(35) Haggenmueller, R.; Rahatekar, S. S.; Fagan, J. A.; Chun, J.; Becker, M. L.; Naik, R. R.; Krauss, T.; Carlson, L.; Kadla, J. F.; Trulove, P. C.; Fox, D. F.; DeLong, H. C.; Fang, Z.; Kelley, S. O.; Gilman, J. W. *Langmuir* **2008**, *24*, 5070–5078.
(36) Vaisman, L.; Wagner, H. D.; Marom, G. *Adv. Colloid Interface Sci.* **2006**, *128−130*, 37–46.
(37) Arnold, M. S.; Green, A. A.; Hulvat, J. F.; Stupp, S. I.; Hersam, M. C. *Nat. Nanotechnol.* **2006**, *1*, 60–65.
(38) Crochet, J.; Clemens, M.; Hertel, T. *Phys. Status Solidi B* **2007**, *244*, 3964–3968.
(39) Miyata, Y.; Yanagi, K.; Maniwa, Y.; Kataura, H. *J. Phys. Chem. C* **2008**, *112*, 3591–3596.
(40) Wei, L.; Wang, B.; Goh, T. H.; Li, L.-J.; Yang, Y.; Chan-Park, M. B.; Chen, Y. *J. Phys. Chem. B* **2008**, *112*, 2771–2774.
(41) Schmidt, C. D.; Bottcher, C.; Hirsch, A. *Eur. J. Org. Chem.* **2007**, 5497–5505.
(42) Tomonari, Y.; Murakami, H.; Nakashima, N. *Chem. Eur. J.* **2006**, *12*, 4027–4034.
(43) Guldi, D. M.; Rahman, G. M. A.; Jux, N.; Tagmatarchis, N.; Prato, M. *Angew. Chem., Int. Ed.* **2004**, *43*, 5526–5530.
(44) Sgobba, V.; Rahman, G. M. A.; Guldi, D. M.; Jux, N.; Campidelli, S.; Prato, M. *Adv. Mater.* **2006**, *18*, 2264–2269.
(45) Mateo-Alonso, A.; Ehli, C.; Chen, K. H.; Guldi, D. M.; Prato, M. *J. Phys. Chem. A* **2007**, *111*, 12669–12673.

carboxy{9-cascade: aminomethane[3]:(2-aza-3-oxypentylidyne): propionic acid}pentyl)perylene-3,4,9,10-tetracarboxybisimide), and **3** (*N*-(5-carboxy{9-cascade: aminomethane[3]:(2-aza-3-oxypentylidyne): propionic acid}pentyl)-*N*′-(dodecyl)perylene-3,4,9,10-tetracarboxybisimide) (0.01 wt% as well as 0.1 wt%) were added to yield SWCNT concentrations of 0.05 g/L, 0.1 g/L, 0.25 g/L, 0.33 g/L, and 0.50 g/L. The resulting mixture was sonicated for 30 min with the aid of an ultrasonic bath and centrifuged for 30 min at 15 000 rpm unless otherwise noted. For the stepwise addition of the aqueous solution of SDBS, 10−30 μL portions of a solution of SDBS (0.5 wt%) were added to 2 mL of a buffered solution of SWCNT−Per3 ($[SWCNT]_i$ = 0.25 g/L, $[Per]_i$ = 0.1 wt%) after centrifugation. To ensure homogeneity, the resulting solution was sonicated for 20 min before the acquisition of the nanotube fluorescence.

Results and Discussion

In this study three different perylene derivatives (**1**−**3**) have been investigated with respect to their dispersion behavior of SWCNTs in aqueous media. Water solubility of the perylene derivatives is ensured by peripheral dendronization with 1G- and 2G-Newkome[46] dendrons. Perylenes **1** and **2** are both symmetrically equipped with two 1G- and 2G-Newkome dendrons, respectively. In contrast, Per3 is asymmetrically substituted in the periphery. The bola-amphiphiles **1** and **2** have shown to form less regular micelles compared to the asymmetric perylene bisimide **3**.[41] The 1G-analogue of **3** remains insoluble in buffered water because of insufficient overall hydrophilicity.[41] To the best of our knowledge, no investigations concerning dispersion of nanotubes in aqueous media by perylene bisimide derivatives have been reported so far, presumably because water-soluble perylene derivatives are not readily available. However, the synthesis and characterization of the outstanding properties of the three highly water-soluble perylene bisimide derivatives used in this study has recently been published by our group.[41]

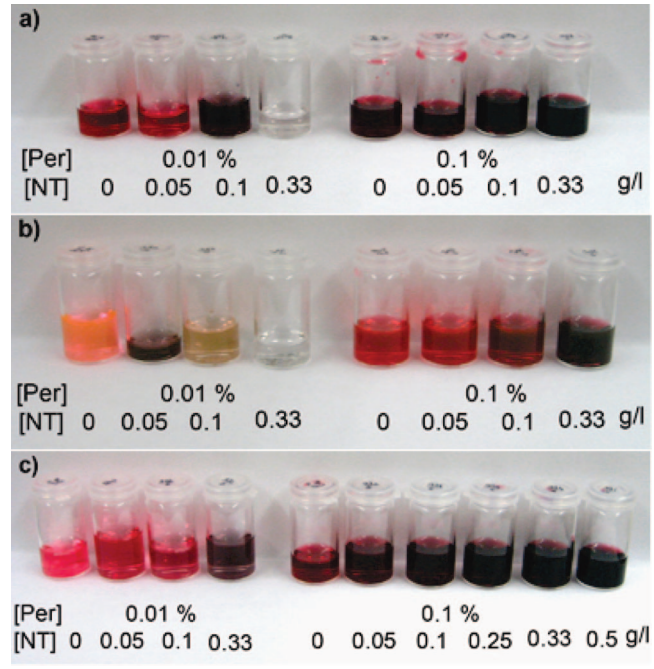

Figure 1. Photographs of SWCNT−Per solutions (a) SWCNT−Per1, (b) SWCNT−Per2, (c) SWCNT−Per3 after centrifugation.

The solubilization of HiPco SWCNTs[47] by the water-soluble perylene bisimide derivatives **1**−**3** was carried out according to the following procedure: varying amounts of raw SWCNTs were dispersed by sonication[48,49] (30 min) in an aqueous solution of the perylene derivatives (phosphate buffer, pH = 7) with the concentrations 0.01 wt% and 0.1 wt%, respectively. The resulting dispersions were centrifuged (15 000 rpm, 30 min) to yield the corresponding SWCNT

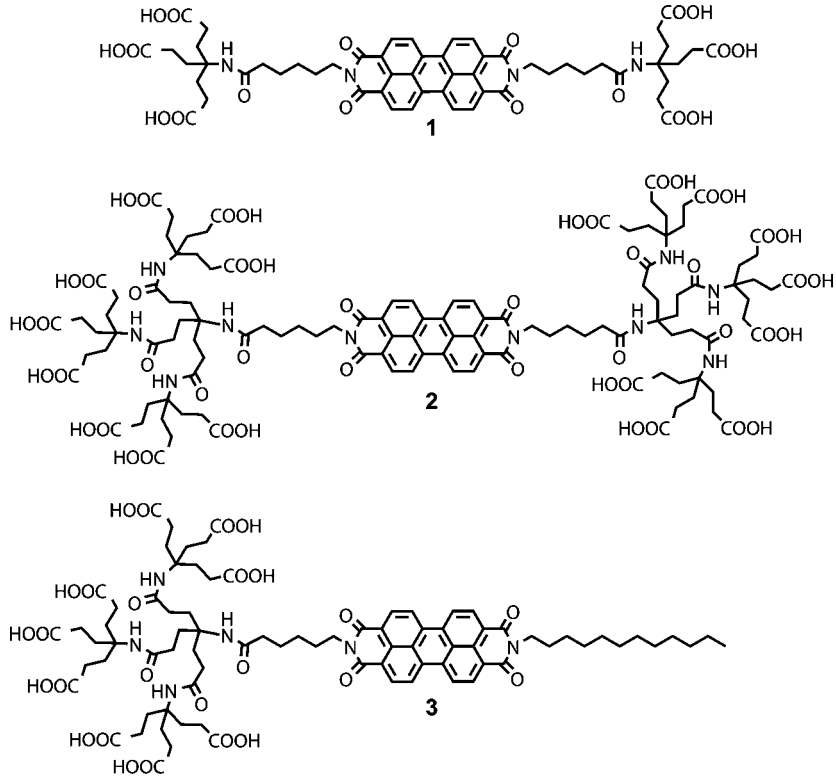

solutions SWCNT−Per1−3. Figure 1 depicts the photographs of SWCNTs dispersed in aqueous solutions of the three different amphiphilic perylene derivatives (SWCNT−Per1−3). It can be estimated by eye that a significant uptake of SWCNTs into aqueous solution has taken place, as the solutions compared to the perylene solution without nanotubes are significantly darkened. The resulting dispersions have been stable for weeks without the observation of any visible precipitation. In some cases, however, the solutions appear completely colorless, e.g. when the concentration of the nanotubes is high (0.33 g/L) and the concentration of perylene low (0.01 wt%). With this high excess of SWCNT material, presumably the perylene molecules are completely adsorbed onto the SWCNT surface without being able to disperse them, as a critical ratio of surfactant concentration to nanotube concentration has to be exceeded in the dispersion of SWCNTs.

By subsequently adding an aqueous solution of perylene **3** to SWCNTs in buffer solution (pH = 7), the nanotube dispersion becomes homogeneous upon sonication when the ratio of the perylene to nanotube concentration [Per3]:[SWCNT] is higher than 1:3.4. The corresponding UV/vis/nIR absorption spectrum is displayed in Figure S1, Supporting Information. The first individualized nanotubes are observed by fluorescence spectroscopy (see Figure S2, Supporting Information), when the ratio [Per3]:[SWCNT] is 1:2.1.

It shall be mentioned that the concentration of the solution of the perylene is kept low, however, above the critical micelle concentration (cmc), compared to usual surfactant concentrations ranging from 0.5 wt% to 2 wt%.[28,32] This is due to the strong optical absorption and emission of the perylene chromophore which overlaps with the absorption and emission of the SWCNT material. Thus, an accurate characterization of the SWCNT−perylene aggregates and their underlying interaction is only possible for lower initial concentrations (0.01 wt% and 0.1 wt%) of perylene in buffered water.

Even though a significant amount of SWCNTs is disperseable in buffered aqueous solutions of the three different perylene bisimide derivatives **1**−**3**, we will focus on the amphiphilic perylene **3** in the following, as amphiphilic molecules forming very stable micelle structures have shown to be very effective surfactants in the dissolution and exfoliation of SWCNTs.[27]

Optical absorption spectra were collected for the solutions after precipitation, as well as after centrifugation. In the case of the samples referred to as "precipitated" we did not apply centrifugation and merely allowed the nondispersed material to settle down for one week prior to the acquisition of the spectra. A comparison of the absorption spectra of the supernatant solutions of precipitation and centrifugation experiment correlates with the overall amount of nanotubes dispersed (including larger bundles) for the precipitated samples and the amount of small bundles and individual tubes for the centrifuged samples, as larger bundles are removed from the dispersion by the centrifugation process. Figure 2 shows the UV/vis/nIR

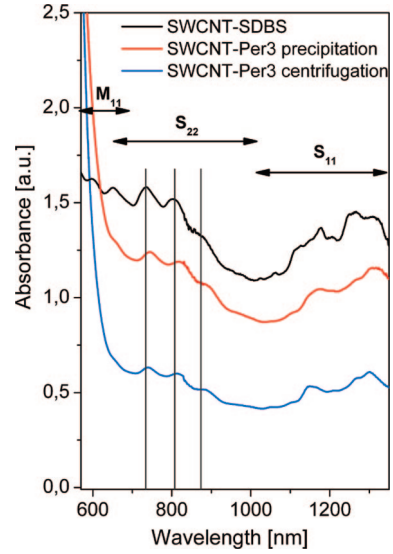

Figure 2. UV/vis/nIR absorption spectra of a buffered aqueous solution of SWCNT−Per3 compared to SWCNT dispersed in SDBS (1 wt%) after precipitation, as well as after centrifugation, $[SWCNT]_i = 0.25$ g/L, $[Per]_i = 0.1$ wt%.

spectra of the SWCNT−Per3 composite after precipitation, as well as after centrifugation compared to the spectra of SWCNTs dispersed in an aqueous solution of the ionic surfactant sodium dodecylbenzenesulfonate ([SDBS] = 1 wt%) after centrifugation. The same process parameters (initial SWCNT concentration: $[SWCNT]_i = 0.25$ g/L, sonication power and time, centrifugation conditions) were utilized in order to ensure comparability. SDBS is a commonly used surfactant aiding the dispersion of SWCNTs in water and is known to yield well resolved SWCNT absorption and emission features.[27,30−35,40,50] However, dispersion and individualization of SWCNTs has shown to be most effective for SDBS concentration of 1 wt%[31] which is 10-fold higher than the concentrations of the perylenes.

It is important to note that the characteristic features arising from the interband transitions between the mirror image spikes in the density of states of the SWCNTs in SWCNT-Per3 (van-Hove-singularities, vHS) are discernible, clearly indicating that the darkening of the perylene solution is due to the uptake of nanotubes. According to Coleman and co-workers[51,52] concentrations of nanotubes in dispersions after precipitation and after centrifugation, respectively, can be calculated from the initial SWCNT concentration as follows:

$$[SWCNT] = [SWCNT]_i A/A_i$$

where [SWCNT] represents the carbon nanotube concentration in dispersion, A is the absorption intensity at a specific, fixed wavelength and the index i denotes the initial concentration and the related initial absorption intensity.

It is important to note that at nanotube concentrations exceeding 0.25 g/L, the detection limit of the spectrometer is reached and therefore the exact determination of the SWCNT concentration cannot be applied to this concentration regime. Nevertheless, the method established by Coleman et al.[51,52] can easily be adopted to our precipitation and centrifugation experiment in order to quantify the actual SWCNT concentrations.

(46) Newkome, G. R.; Moorefield, C. N.; Vögtle, F. *Dendritic Molecules: Concepts, Syntheses, Perspectives*; VCH: Weinheim, 1996.
(47) Nikolaev, P.; Bronikowski, M. J.; Bradley, R. K.; Rohmund, F.; Colbert, D. T.; Smith, K. A.; Smalley, R. E. *Chem. Phys. Lett.* **1999**, *313*, 91–97.
(48) Niyogi, S.; Hamon, M. A.; Perea, D. E.; Kang, C. B.; Zhao, B.; Pal, S. K.; Wyant, A. E.; Itkis, M. E.; Haddon, R. C. *J. Phys. Chem. B* **2003**, *107*, 8799–8804.
(49) Grossiord, N.; Regev, O.; Loos, J.; Meuldijk, J.; Koning, C. E. *Anal. Chem.* **2005**, *77*, 5135–5139.
(50) McDonald, T. J.; Engtrakul, C.; Jones, M.; Rumbles, G.; Heben, M. J. *J. Phys. Chem. B* **2006**, *110*, 25339–25346.
(51) Giordani, S.; Bergin, S. D.; Nicolosi, V.; Lebedkin, S.; Kappes, M. M.; Blau, W. J.; Coleman, J. N. *J. Phys. Chem. B* **2006**, *110*, 15708–15718.

Table 1. Tabulated Absorption Intensity at 735 nm and Calculated Nanotube Concentrations According to Eq 1[a]

$[SWCNT]_i$	A_i [a.u.]	A_{pr} [a.u.]	A_{cf} [a.u.]	$[SWCNT]_{pr}$	$[SWCNT]_{cf}$
[Per3] = 0.01 wt%					
0.05 g/L	0.713	0.249	0.036	0.017 g/L (35%)	0.0025 g/L (5%)
0.1 g/L	1.543	0.595	0.066	0.038 g/L (38%)	0.0043 g/L (4%)
[Per3] = 0.1 wt%					
0.05 g/L	0.459	0.366	0.160	0.039 g/L (80%)	0.017 g/L (35%)
0.1 g/L	1.074	0.478	0.313	0.045 g/L (44%)	0.029 g/L (29%)
0.25 g/L	2.779	1.240	0.632	0.111 g/L (44%)	0.057 g/L (23%)
[SDBS] = 1 wt%					
0.05 g/L	1.540	1.303	0.596	0.042 g/L (85%)	0.019 g/L (38%)
0.1 g/L	2.620	2.207	0.667	0.084 g/L (84%)	0.025 g/L (25%)

[a] $[SWCNT]_i$, initial SWCNT concentration; A_i, initial absorption intensity (735 nm); A_{pr}, absorption intensity after precipitation (735 nm); A_{cf}, absorption intensity after centrifugation (735 nm); $[SWCNT]_{pr}$, calculated SWCNT concentration after precipitation; $[SWCNT]_{cf}$, calculated SWCNT concentration after centrifugation.

Contrary to original work[51,52] we have chosen the S_{22}-transition at 735 nm for the determination of the absorption intensities and calculation of the SWCNT concentrations as the absorption of the free bulk perylene covers the excitation region from 400−650 nm. Quantitative values for SWCNT concentrations after precipitation as well as after centrifugation are given in Table 1. As can be seen, there is a clear dependence of the Per3 concentration on the amount of SWCNTs dispersed by this amphiphilic surfactant. For instance, with an initial nanotube concentration of 0.1 g/L, 38% of the nanotubes remain dispersed in a 0.01 wt% solution of Per3 after precipitation opposed to 44% for a 0.1 wt% solution of Per3. The difference is more striking for the material after centrifugation, as merely 4% of the nanotubes remain in the 0.01 wt% Per3 solution, whereas 29% of the nanotubes are still present after centrifugation in the 0.1 wt% Per3 solution.

This portion is even higher than SWCNT concentration in a 1 wt% solution of SDBS (25%) under equal experimental conditions. Thus, most remarkably, an aqueous solution of the perylene bisimide **3** at 0.1 wt% is capable of dispersing a higher portion of SWCNTs compared to a solution of SDBS at 1 wt% after centrifugation. This underlines the potential surfactant ability of the investigated perylene derivative **3**.

Upon comparison of the spectra of SWCNTs dispersed in an aqueous solution of the perylene to SWCNTs dispersed in an aqueous solution of SDBS, a red-shift of the vHS is clearly discernible as well as peak broadening in the nIR region (first order semiconducting transitions, S_{11}), presumably due to adsorption of the extended π-electron system of the perylene derivative onto the SWCNT backbone and therefore electronic interaction.

Upon adsorption of the aromatic perylene unit, the position of the $\pi-\pi^*$ and $n-\pi^*$ transitions of the perylene is also expected to be different. However, this is only observed when the concentration of free perylene in the solution is kept as low as possible to reduce overlapping of the signals of free perylene and nanotube bound perylene. Figure 3 depicts the UV/vis absorption spectra of a buffered aqueous solution of Per3 (0.01 wt%) compared to the spectra of two different concentrations of nanotubes ($[SWCNT]_i = 0.0043$ g/L and $[SWCNT]_i = 0.031$ g/L) dispersed in the solution of Per3 after centrifugation. The strong absorption peaks centered at 500 and 542 nm are attributed to the $\pi-\pi^*$ and $n-\pi^*$ transitions of the perylene unit, respectively. The peaks do not appear shifted in the sample with a lower nanotube concentration (red trace), suggesting that this spectrum is governed by **3** in the bulk solution. Upon increasing the concentration of nanotubes in an aqueous solution of Per3, more perylene is bound to the surface of the nanotube therefore reducing the concentration of free perylene. In this case (blue trace), the $\pi-\pi^*$ and $n-\pi^*$ transitions of the perylene unit appear at 508 and 550 nm. This red-shift of 8 nm relative to the original aqueous perylene solution further emphasizes π-interaction between the aromatic perylene core of **3** and the surface of the SWCNT.

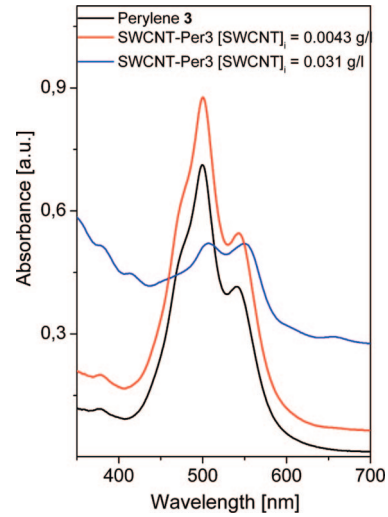

Figure 3. UV/vis absorption spectra of SWCNTs at two different concentrations ($[SWCNT] = 0.0043$ g/L and $[SWCNT] = 0.031$ g/L) dispersed by an aqueous solution of Per3 after centrifugation compared to the absorption spectra of the corresponding perylene solutions without nanotubes ($[Per]_i = 0.01$ wt%).

As described elsewhere, a buffered aqueous solution of Per3 ($[Per] = 0.01$ wt%) shows absorption spectra with typical bands for self-aggregated perylene dyes being characterized by a more intense $\pi-\pi^*$ transistion compared to the $n-\pi^*$ transition.[41,53] However, the spectral features of the perylene unit in SWCNT−Per3 (blue trace in Figure 3) is rather indicative for a significantly lower degree of self-aggregation between the perylene moieties, as the $n-\pi^*$ transition becomes more intense. This further supports the conclusion that the perylene molecules are adsorbed on the nanotube surface, therefore reducing self-aggregation. As discussed in the section above, optical absorp-

(52) Nicolosi, V.; Cathcart, H.; Dalton, A. R.; Aherne, D.; Dieckmann, G. R.; Coleman, J. N. *Biomacromolecules* **2008**, *9*, 598–602.

(53) Wuerthner, F. *Chem. Commun.* **2004**, 1564–1579.

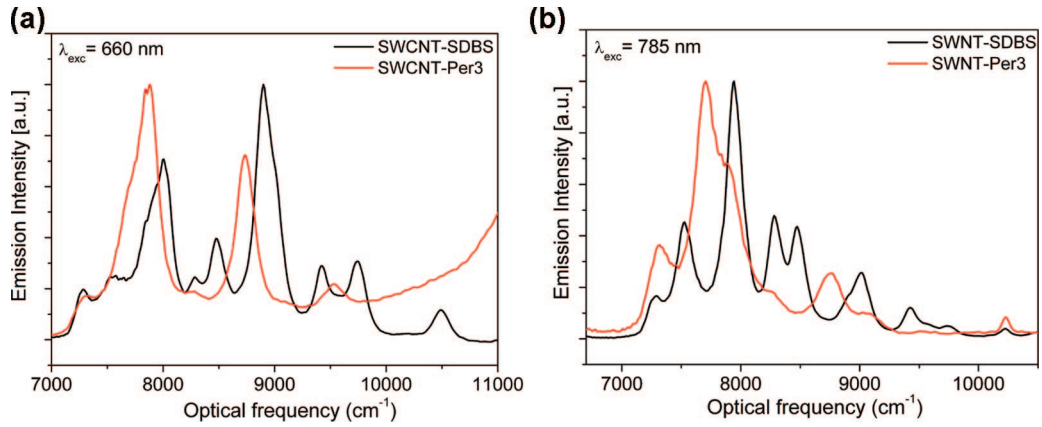

Figure 4. Fluorescence spectra of SWCNT−Per3 compared to SWCNT dispersed in SDBS (1 wt%) after centrifugation, [SWCNT] = 0.057 g/L, $[Per]_i$ = 0.1wt% with (a) λ_{exc} = 660 nm and (b) λ_{exc} = 785 nm. All spectra were normalized to the highest emission feature.

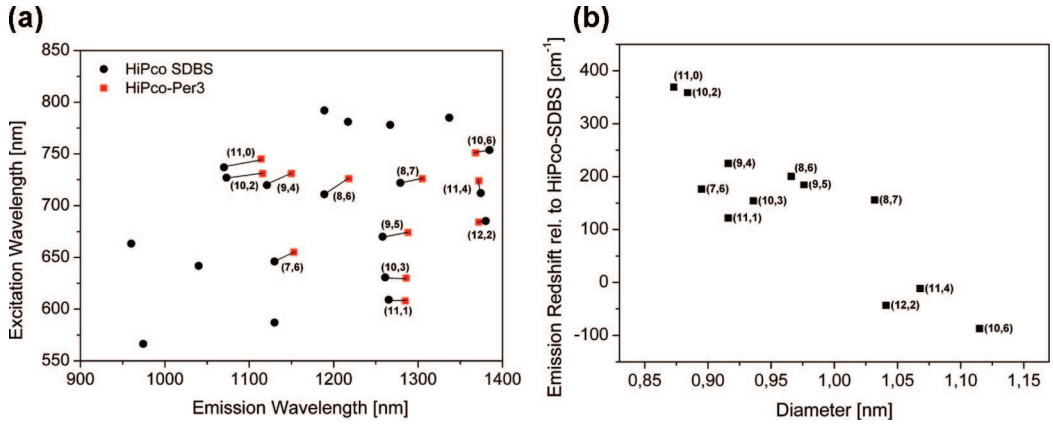

Figure 5. (a) Plot for optical transitions for Per3 (red squares) and SDBS (black dots) dispersed nanotubes extracted from the photoluminescence excitation maps (Figure S3, Supporting Information); (b) relation of the magnitude of the emission peak shift to the diameter of the nanotubes. Positive values denote a red-shift, while negative values correspond to a blue-shift.

tion spectroscopy demonstrates that SWCNTs are well dispersable in an aqueous solution of the perylene bisimide **3** even at low perylene concentrations ($[Per]_i$ = 0.01 wt%). The characteristic absorption features of the SWCNTs (vHS) appear red-shifted, as well as the $\pi-\pi^*$ and $n-\pi^*$ transitions of the perylene unit, strongly indicating $\pi-\pi$-stacking interaction between the perylene unit and the nanotube surface. To further investigate the aggregation state of the nanotubes in solution, fluorescence spectroscopic measurements have been carried out, as only individualized semiconducting SWCNTs contribute intensity.

NIR emission spectroscopy is a powerful tool in nanotube characterization especially when the aggregation state is to be investigated,[28,33,38,50,54] as fluorescence is obtained directly across the band gap of semiconducting nanotubes.[26,55,56] Therefore, fluorescence is substantially broadened or quenched in SWCNT bundles through interaction with metallic SWCNTs.[26] Thus, merely individualized semiconducting SWCNTs are detected. The emission spectra of the SWCNT−Per3 solutions were recorded at two different excitation wavelengths λ_{exc} = 660 nm and λ_{exc} = 785 nm exciting the first-order semiconducting transitions (S_{11}) and the second-order semiconducting transitions (S_{22}), respectively. Figure 4 shows the normalized fluorescence spectra of SWCNT−Per3 in comparison to SWCNTs dispersed in a solution of SDBS ([SWCNT] = 0.057 g/L). SWCNT−Per3 shows fluorescence signals clearly revealing that SWCNTs are not only dispersed but also individualized by the perylene derivative. The broad emission onset in the high frequency region of the solution of SWCNT−Per3 with λ_{exc} = 660 nm is attributed to the fluorescence of the perylene unit. It shall further be mentioned that the fluorescence signals in the case of the perylene dispersed nanotubes appear at different positions compared to nanotubes dispersed by SDBS[50] because of the differing surrounding of the nanotubes influencing the electronic structure and therefore their absorption and emission properties.

To account for the attenuation of the emission pattern, 3D photoluminescence excitation maps were recorded for SWCNT dispersed in an aqueous solution of SDBS (Figure S3a, Supporting Information) and for SWCNT−Per3 (Figure S3a, Supporting Information). Figure 5a illustrates the magnitude of the perylene induced shifts (red squares) on the optical transitions of the semiconducting SWCNTs compared to nanotubes dispersed in SDBS (black dots). The shifts span from 87 cm^{-1} blue-shift to 369 cm^{-1} red-shift. Upon closer inspection, a relationship between the emission peak shift and the diameter of the nanotube was found, as depicted by Figure 5b.

(54) Yoon, D.; Kang, S.-J.; Choi, J.-B.; Kim, Y.-J.; Baik, S. *J. Nanosci. Nanotechnol.* **2007**, *7*, 3727–3730.
(55) Bachilo, S. M.; Strano, M. S.; Kittrell, C.; Hauge, R. H.; Smalley, R. E.; Weisman, R. B. *Science* **2002**, *298*, 2361–2366.
(56) Weisman, R. B.; Bachilo, S. M.; Tsyboulski, D. *Appl. Phys. A: Mater. Sci. Process.* **2004**, *78*, 1111–1116.

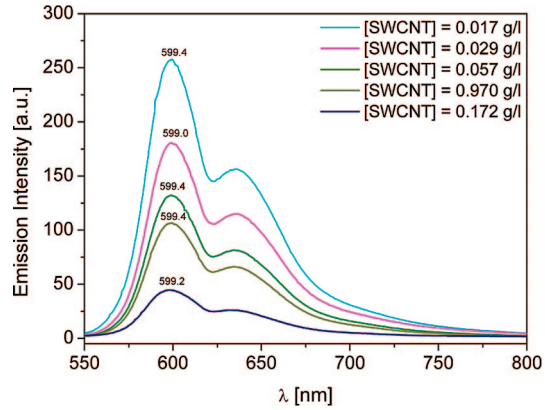

Figure 6. Fluorescence emission spectra of aqueous solutions of SWCNT−Per3 with $\lambda_{exc} = 500$ nm at different SWCNT concentrations.

The SWCNTs with a diameter larger than 1.05 nm exhibit a slight blue-shift, opposed to the red-shift of the emission features for smaller diameter nanotubes. More specifically, the emission of the (11,0) and (10,2) SWCNTs is red-shifted by approximately 43 nm (360 cm^{-1}). This behavior strongly supports the conclusion that there is communication between the nanotube and the adsorbed perylene derivative, even though further investigations are deemed necessary to specify the nature of the interaction.

To further elucidate the effects of the adsorption of Per3 to the nanotube sidewall, emission spectroscopy was also carried out upon excitation of the perylene ($\lambda_{exc} = 500$ nm) moiety in an aqueous solution of Per3 (0.01 wt%) with varying concentrations of SWCNTs. The fluorescence of Per3 is shown to be subsequently quenched when increasing the amount of SWCNTs as depicted by figure 6. This is attributed to the fact that upon increasing the amount of SWCNTs in a solution of perylene, the amount of free perylene responsible for the emission after excitation with $\lambda_{exc} = 500$ nm is decreased, as more perylene is adsorbed on the surface of the nanotube. The $\pi-\pi$ stacking interaction of the tubes with the adsorbed perylene, being an electron poor aromatic molecule, provides an ideal scenario for electronic communication between the two electrophores, such as photoinduced energy or electron transfer, which in both cases explains the observed fluorescence quenching. In addition, an inner-filter effect[34] of the nanotubes could also contribute to the observed decrease of emission intensity. Elimination of the inner-filter effect in this experiment is not trivial, as the usual methodology to overcome this problem involves dilution of the samples to the same nanotube concentrations. However, diluting the SWCNT−Per3 dispersions would also result in alteration of the perylene fluorescence, as the emission of **3** is highly dependent on the aggregation state of the perylene. A concentration-dependent fluorescence study of Per3 revealed that the emission intensity reaches a maximum at concentrations of approximately 5×10^{-5} M. At higher concentrations, however, the fluorescence is subsequently quenched because of the self-aggregation of the perylene moieties.[41]

In summary, the nIR emission spectroscopic investigations reveal that fluorescence of the nanotubes is not completely quenched by the adsorption of the perylene moieties in the case of SWCNT−Per3 and therefore indicating that individualization of nanotubes has occurred. For further investigation of the degree of bundling/individualization of the nanotubes dispersed in an aqueous solution of Per3, microscopic techniques have been employed.

Statistical atomic force microscopy (AFM) analysis was performed in order to compare the degree of individualized nanotubes in an aqueous solution of Per3 to an aqueous solution of SDBS. Figure 7 shows representative AFM images of the SWCNT−Per3 supernatant (Figure 7a, top) as well as of the SWCNT−SDBS supernatant (Figure 7b, top) after spin coating. In the lower section the corresponding height profiles are displayed. The concentrations of perylene and SWCNTs had to be chosen with care, as it is desirable to keep the amount of free perylene low in order to reduce the population of perylene micelles overlapping with the SWCNT structures. Therefore, a surfactant concentration of 0.01 wt% was used. To ensure maximum loading of SWCNTs in the solutions of 0.01 wt% perylene, the sample with the highest absorption intensity in the UV/vis/nIR spectra was investigated by AFM ([SWCNT] = 0.031 g/L).

The AFM images of SWCNT−Per3 (Figure 7a) confirm the conclusion drawn from the fluorescence spectra, as individual SWCNTs are observed besides small bundles. This nicely demonstrates the ability of Per3 not only to disperse but also to individualize SWCNTs in water to a high degree even at very low surfactant concentrations.

A detailed height analysis of the SWCNTs bundles and individual tubes was also performed by AFM from the spin-coated dispersions of nanotubes in a solution of Per3 and SDBS, respectively. It has to be mentioned that the diameters do not appear completely uniform along the lengths of the carbon nanotubes, as, presumably, the nanotubes are not uniformly coated by the perylene so that areas of bare SWCNTs are observed along with surfactant-coated areas. The lengths of the individual and bundled SWCNTs range from 20 nm to several μm.

The diameter measurements were obtained from 50 AFM images at multiple points along each carbon nanotube bundle. Figure 8 shows the histograms of the bundle diameter distribution derived from the AFM analysis on SWCNTs dispersed in a solution of Per3 and SDBS, respectively. Statistical analysis shows that 35% of the SWCNTs are present as individual tubes when being dispersed in a buffered aqueous solution of **3**. Another 43% of the SWCNTs are aggregated in small bundles of up to 5 nm in diameter which corresponds to bundles of up to 5 individual tubes, while merely the residual 22% are arranged in medium size or large bundles. In contrast, SWCNTs being immersed in an aqueous solution of the widely used surfactant SDBS shows a much wider bundle diameter distribution and a significantly lower degree of individualization under the same conditions: 14% of the nanotubes appear individualized, 43% are aggregated in small bundles (diameter of up to 5 nm), and more than half of the SWCNTs (57%) form bundles with diameters greater than 5 nm. The statistical AFM analysis reveals that a buffered aqueous solution of Per3 is capable of individualizing SWCNTs to a higher degree compared to an aqueous solution of SDBS under equal experimental conditions even though AFM is measured on air-dried samples where surface adhesion may cause the nanotubes to reagglomerate.

In order to further elucidate the aggregation state of the CNTs in solution[32,49] vitrified samples were imaged by the cryo-TEM technique. Figure 9 depicts cryo-TEM images of SWCNTs dispersed in a buffered aqueous solution of Per3, as well as SWCNTs dispersed in an aqueous solution of SDBS.

In contrast to AFM, a high concentration of SWCNTs in solution is desired in order to facilitate the measurement. Thus, a nanotube concentration of 0.243 g/L for SWCNTs dispersed in a solution of SDBS and a concentration of 0.172 g/L for

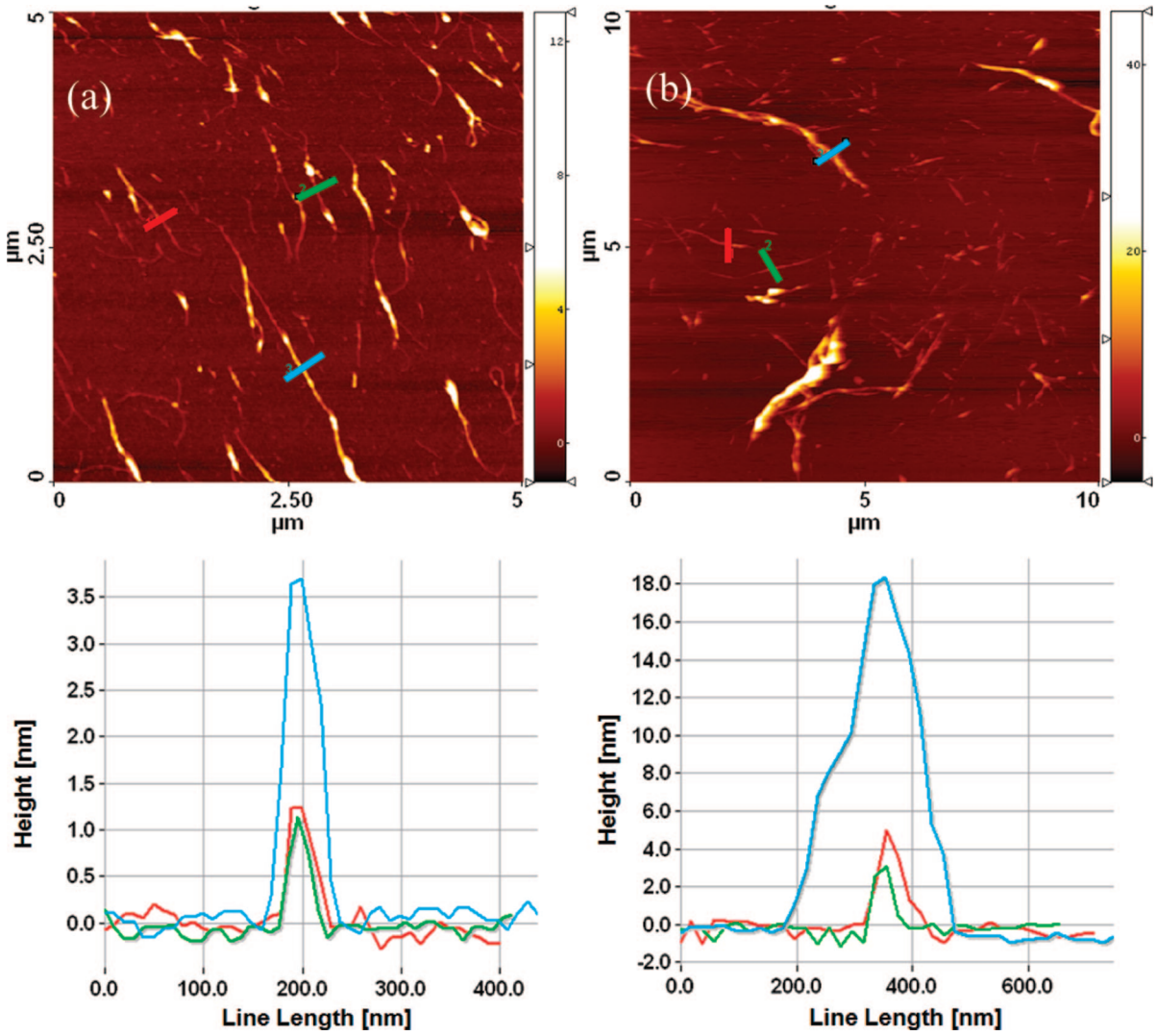

Figure 7. (a) Representative AFM image of SWCNT−Per3 (top) ($[Per]_i = 0.01$ wt%, [SWCNT] = 0.031 g/L), (b) representative AFM image of SWCNT dispersed in a solution of SDBS (top) ($[SDBS]_i = 0.01$ wt%, [SWCNT] = 0.020 g/L) after spin coating the supernatant of the centrifuged samples and the corresponding height profile (bottom).

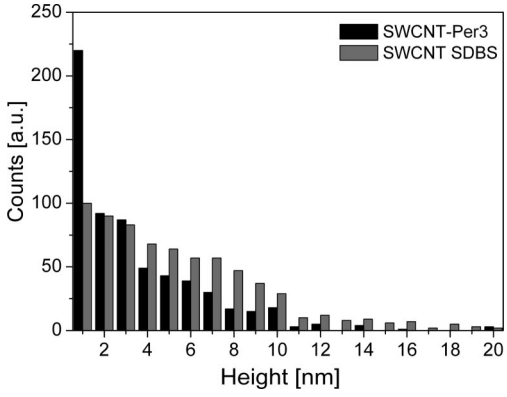

Figure 8. Histogram of bundle diameter obtained by AFM analysis of aqueous solutions of SWCNTs dispersed in **3** and a solution of SDBS after spin coating the supernatant after centrifugation.

SWCNT−Per3 was used. As shown by previous cryo-TEM investigations on nanotubes,[25,32,49,57,58] the SWCNT aggregates appear to be extraordinarily straight and long (up to several μm in length) compared to an atomic force microscopic view, where nanotubes tend to coil up because of surface adhesion with the wafer upon drying. The SWCNTs dispersed in SDBS appear as partly individualized tubes, along with bundles of up to 20 tubes (Figure 9a and 9b). In contrast, the nanotubes in SWCNT−Per3 appear to be individualized to a higher degree (Figure 9c and 9d). The overall bundle size is also reduced (about five individual tubes). In both cases, surfactant micelles are observed in the background.

Besides, the sidewalls of the nanotubes are decorated with small particles of high density. Presumable, those are iron catalyst impurities present in the untreated SWCNT material.[25,49,57,58] An investigation concerning dispersion of SWCNTs in various surfactants by Moore et al.[32] has revealed via cryo-TEM imaging that the amount of the catalytic impurities is drastically reduced by ultracentrifugation. Remarkably, the amount of catalyst particles adsorbed on the SWCNT surface appears to be strongly reduced in SWCNT−Per3 compared to SWCNT dispersed in a solution of SDBS without the need for ultracentrifugation,

(57) Dror, Y.; Pyckhout-Hintzen, W.; Cohen, Y. *Macromolecules* **2005**, *38*, 7828–7836.

(58) Bandyopadhyaya, R.; Nativ-Roth, E.; Regev, O.; Yerushalmi-Rozen, R. *Nano Lett.* **2002**, *2*, 25–28.

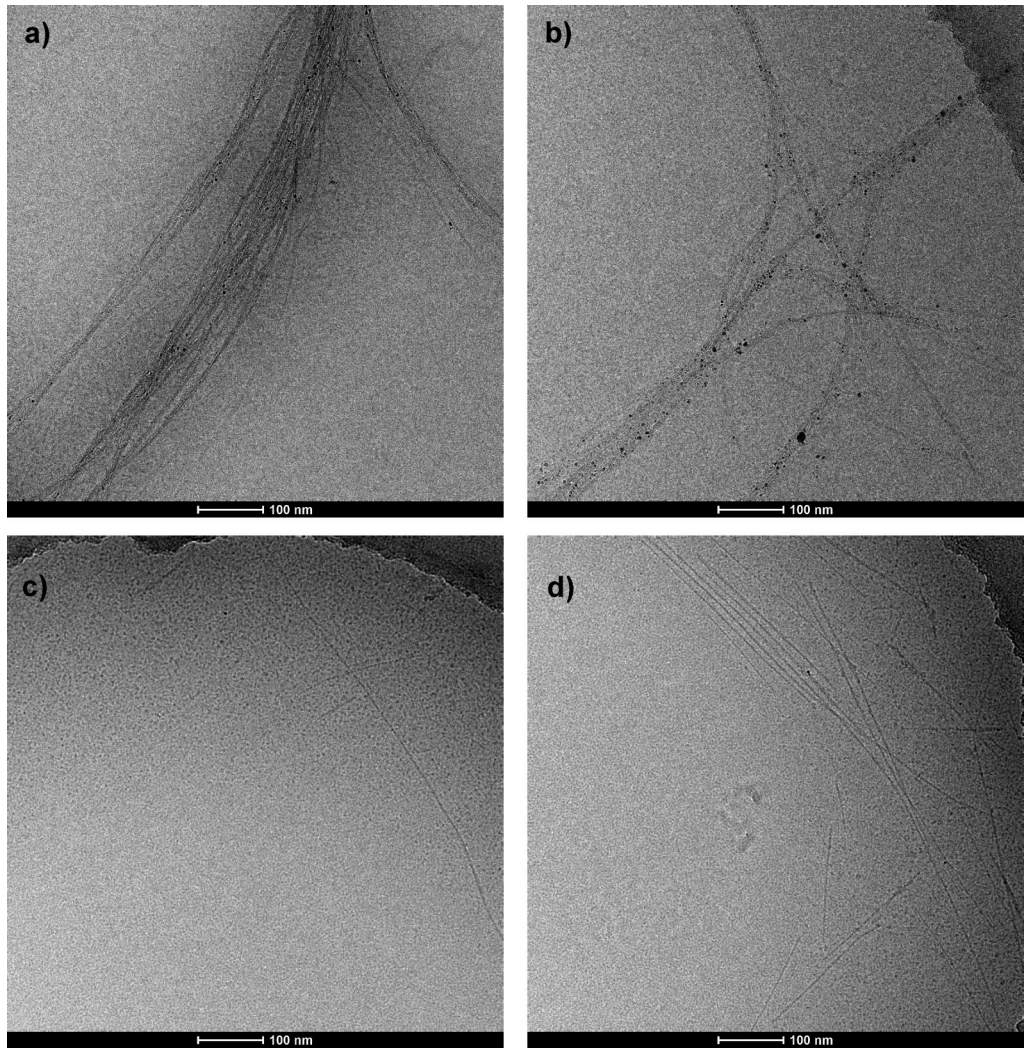

Figure 9. Representative cryo-TEM images of (a, b) SWCNT dispersed in SDBS ([SWCNT] = 0.243 g/L, $[SDBS]_i$ = 1 wt%) and (c, d) SWCNT−Per3 ([SWCNT] = 0.172 g/L, $[Per]_i$ = 0.1 wt%). The images were recorded from the supernatant after centrifugation in all cases.

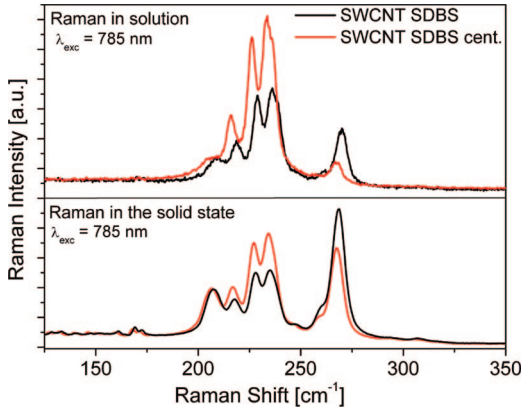

Figure 10. Raman spectra recorded in solution (top) and in the solid state (bottom) (λ_{exc} = 785 nm) of SWCNTs dispersed by SDBS before and after centrifugation. All spectra have been normalized to the G-band (1590 cm^{-1}).

indicating that in the case of Per3, dispersion is restricted to SWCNTs, while a solution of SDBS also disperses a significant amount of impurities.

The microscopic investigations further underscore the potential of the perylene bisimide derivative **3** to act as a surfactant in SWCNT dispersion and indivualization, as a high population of individual nanotubes has been observed by AFM and cryo-TEM. However, further investigations are unambiguous to shed light into the dispersion mechanism.

Since a different dispersion behavior of SWCNTs for solutions of the perylenes is observed in comparison to a solution of SDBS, more detailed investigations concerning the nature of perylene adsorption were performed. For this purpose, a solution of SDBS (0.5 wt%) was added step wisely to a SWCNT−Per3 solution ([SWCNT] = 0.057 g/L, $[Per]_i$ = 0.1wt%) establishing a similar chemical surrounding in the samples (SWCNT−Per3 SDBS). The resulting material was characterized in detail by Raman, UV/vis/nIR, and fluorescence spectroscopy.

As a foundation for the interpretation of the Raman spectra obtained from SWCNT−Per3, first of all, the Raman spectra of the pristine HiPco carbon nanotubes dispersed in an aqueous solution of SDBS shall be discussed. For this purpose, Raman spectra were recorded both in solution and in the solid state (buckypaper) before and after centrifugation of SWCNTs dispersed in a solution of SDBS. The RBM region of the spectra with an excitation wavelength of 785 nm are displayed in Figure 10.

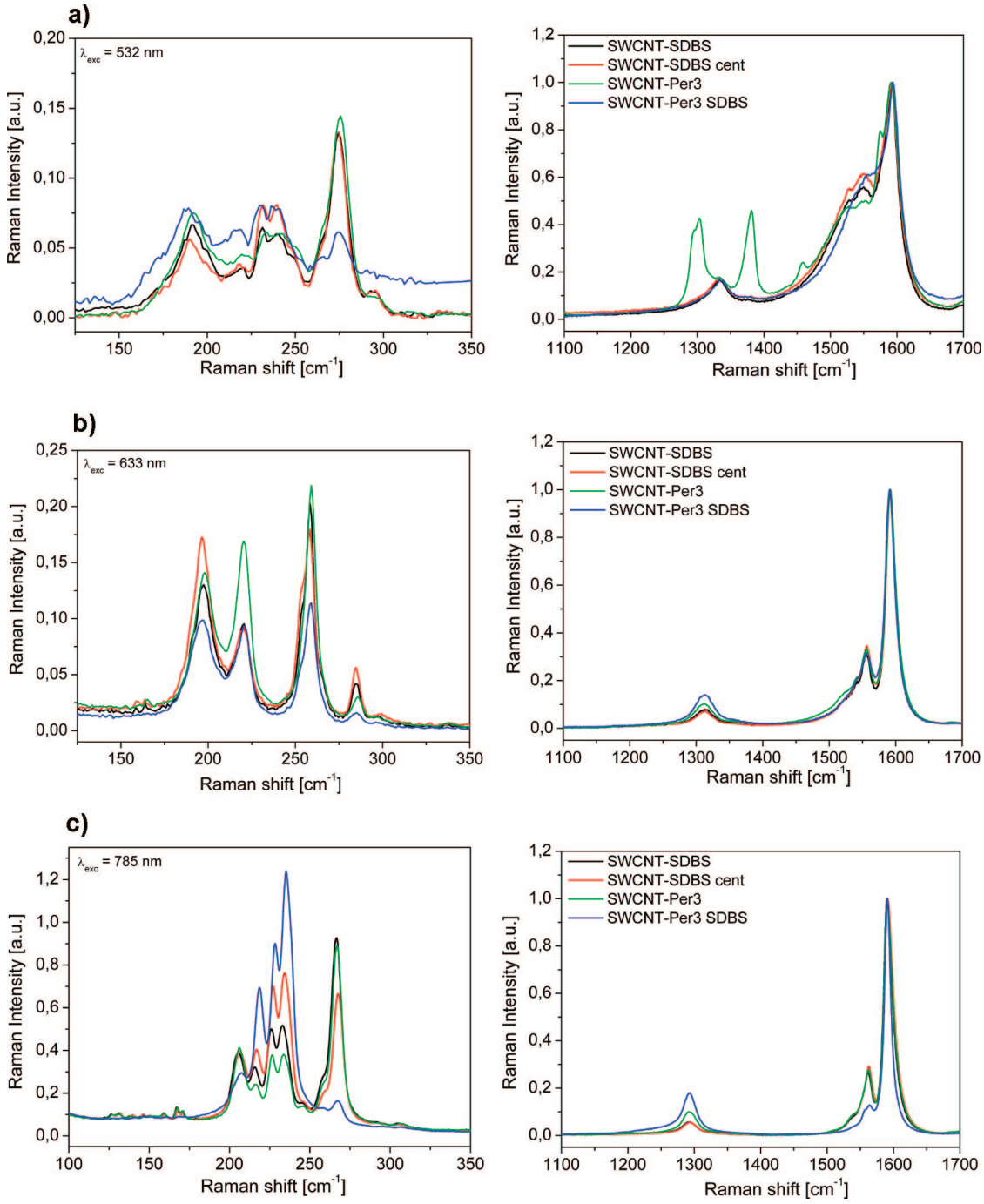

Figure 11. RBM region (left) and region of the tangential modes (right) of the Raman spectra of SWCNT−Per3 compared to SWCNT dispersed in SDBS recorded from the solid, (a) $\lambda_{exc} = 532$ nm, (b) $\lambda_{exc} = 633$ nm, (c) $\lambda_{exc} = 785$ nm. All spectra have been normalized to the G-band (1590 cm^{-1}).

Striking differences have been observed in the relative RBM intensities when comparing the centrifuged to the noncentrifuged material. These changes can be attributed to bundling and debundling phenomena.[59−61] The portion of individual SWCNTs is supposedly higher in the centrifuged material (red trace). This permits the inverse conclusion that larger bundles are present before centrifugation (black trace) inducing a red-shift and larger transition widths of the optical transitions. As Raman spectroscopy on SWCNTs is based on resonance phenomena, an energetic change in the optical transitions has an impact on the RBM structure.

The red-shift brings into resonance different nanotube chiralities in the bundled samples compared to individualized nanotubes. Additionally, broadening gives access to chiralities that have not been within the resonance window of a given excitation wavelength in the narrower band structure of individualized nanotubes.[59−61] Most interestingly, the changes in RBM structure observed from the solution spectra are still present in the spectra recorded on a buckypaper, indicating that even though bundling takes place upon filtration (as can be concluded from the RBM peak at 266 cm^{-1} which is more dominant in spectra of bundled SWCNTs), the structural aspects concerning bundling

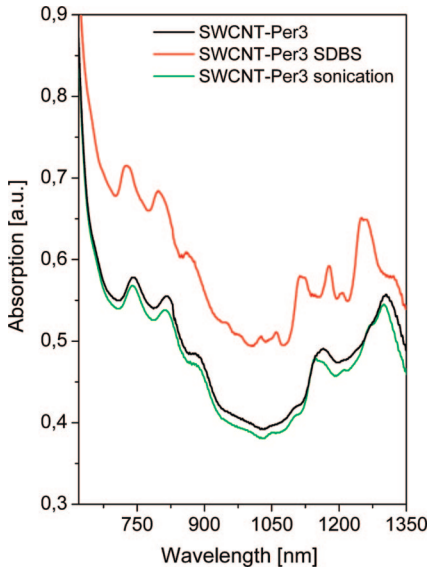

Figure 12. UV/vis/nIR absorption spectra of a buffered aqueous solution of SWCNT−Per3 ([SWCNT] = 0.057 g/L, $[Per]_i$ = 0.1 wt%) before and after addition of an aqueous solution of SDBS; the total amount of SDBS added corresponds to a SDBS concentration of 0.03 wt%.

are preserved. This observation has to be considered when interpreting the Raman spectra of SWCNT−Per3 shown in figure 11. Raman spectra of SWCNT−Per3 were taken from the solid, as the fluorescence of the perylene impedes with the acquisition of the Raman spectra at λ_{exc} = 532 nm and λ_{exc} = 633 nm in solution. The Raman spectra obtained from the solution after excitation with λ_{exc} = 785 nm are totally consistent with the spectra recorded in the solid state (for solution spectra, see Figure S4 in the Supporting Information). Figure 11 displays the Raman spectra of the SWCNT−Per3 composites in the solid state before and after addition of SDBS at three different excitation wavelengths. All spectra were normalized to the G-band (1590 cm^{-1}). As first observation, the Raman modes attributed to the perylene unit at 1308 and 1387 cm^{-1} (λ_{exc} = 532 nm, Figure 11a) are strongly decreased upon the addition of SDBS to SWCNT−Per3 (blue trace). Obviously, SDBS replaces the perylene from the sidewall of the nanotubes so that it is removed in the filtration step. As a consequence, the Raman signals disappear.

A closer investigation of the RBM region reveals that the same structural changes are observed when comparing SWCNT−Per3 SDBS (blue trace) to SWCNTs dispersed in a solution of SDBS after centrifugation (red trace) with SWCNTs dispersed in a solution of SDBS before and after centrifugation (black and red trace, respectively): the feature at 266 cm^{-1} assigned to the (10,2)-SWCNT with a $\nu 2 \rightarrow c2$ optical transition at 734 cm^{-1} becomes partially resonant with the excitation laser at 785 nm in a bundle because of a shift of the interband transition to lower energy. In a highly individualized sample, this feature strongly decreases. Similarly, the intensity of the feature corresponding to the (11,3)-SWCNT at 233 cm^{-1} with $\nu 2 \rightarrow c2$ at 792 cm^{-1} is significantly enhanced. This is totally consistent with the observation of Strano et al. in their investigation on the role of surfactant adsorption during ultrasonication.[62]

The replacement of Per3 from the sidewall of the SWCNT by SDBS is crucial for this comparison, as the same chemical surrounding has to be ensured when discussing bundling and debundling phenomena in spectroscopic investigations. A change in the dielectric environment of the nanotube by adsorption of polyaromatic moieties virtually has the same effect in any type of spectroscopy as a change in the dielectric environment by bundling of nanotubes, albeit to a different extent. This is emphasized by the Raman spectra of SWCNTs dispersed by Per3 before and after addition of SDBS (green and blue trace, respectively): the addition of SDBS to SWCNT−Per3 and therefore replacement of Per3 induces the same changes in relative RBM intensity as debundling.

Absorption spectroscopy also underscores the conclusion drawn from the Raman spectra.[49] Figure 12 displays UV/vis/nIR spectra of SWCNT−Per3 ([SWCNT] = 0.057 g/L, $[Per]_i$ = 0.1wt%) before and after addition of a solution of SDBS. After the addition of a solution of SDBS, an overall SDBS concentration of 0.03 wt% is obtained. To confirm that sonication has a minor impact on the structure of the absorption spectrum, SWCNT−Per3 was further sonicated for 2 h in a blind experiment. Since virtually no difference has been detected, when comparing the sonicated to the initial SWCNT−Per3 solution, obviously further sonication does not increase the degree of debundling without the addition of a solution of SDBS. However, upon addition of SDBS the formerly broadened peaks especially in the region of the S_{11}-transitions appear sharper and shifted to lower wavelength, indicating replacement of the perylene moiety from the sidewall of the nanotubes.

Furthermore, the addition of an aqueous solution of SDBS was mapped by fluorescence spectroscopy. In this case, the stepwise addition is crucial, as subsequent replacement of the perylene molecules adsorbed on the sidewall of the nanotubes by SDBS supposedly results in a stepwise peak shift of the fluorescence signals to obtain spectra similar to pristine SWCNTs in an aqueous solution of SDBS. The resulting emission spectra with λ_{exc} = 660 nm and λ_{exc} = 785 nm are shown in Figure 13a and 13b, respectively.

In contrast to the subsequent peak shift expected, the fluorescence spectra of the nanotubes in perylene solution change drastically to yield spectra similar to SWCNTs in a solution of SDBS, as soon as a certain threshold value of SDBS concentration (0.026 wt%) has been reached. It may be tempting to argue that a certain concentration of SDBS is necessary for the individualization of SWCNTs, as the anionic surfactant SDBS is known to form cylindrical micelles.[30]

However, we found that when adding a solution of SDBS to SWCNT in phosphate buffer (pH = 7) in a blank experiment, individualization starts to occur at SDBS concentrations of 0.01−0.012 wt% which is below the critical micelle concentration (0.046 wt%).[50] The evolution of the fluorescence spectra in the blank experiment (see Supporting Information Figure S5) is governed by a stepwise increase of fluorescence intensity and peak sharpening. McDonald et al.[50] have experimentally determined the stable nanotube suspension concentration by diluting a dispersion of SWCNTs in an aqueous solution of

(59) O'Connell, M. J.; Sivaram, S.; Doorn, S. K. *Phys. Rev. B* **2004**, *69*, 235415/1–235415/15.
(60) Rao, A. M.; Chen, J.; Richter, E.; Schlecht, U.; Eklund, P. C.; Haddon, R. C.; Venkateswaran, U. D.; Kwon, Y. K.; Tomanek, D. *Phys. Rev. Lett.* **2001**, *86*, 3895–3898.
(61) Heller, D. A.; Barone, P. W.; Swanson, J. P.; Mayrhofer, R. M.; Strano, M. S. *J. Phys. Chem. B* **2004**, *108*, 6905–6909.
(62) Strano, M. S.; Moore, V. C.; Miller, M. K.; Allen, M. J.; Haroz, E. H.; Kittrell, C.; Hauge, R. H.; Smalley, R. E. *J. Nanosci. Nanotechnol.* **2003**, *3*, 81–86.

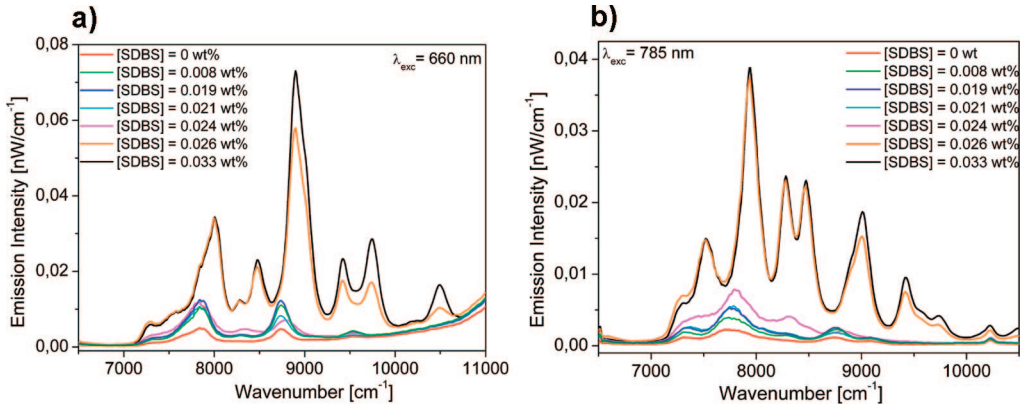

Figure 13. As recorded fluorescence spectra (without normalization) of the addition of SDBS to a buffered aqueous solution of SWCNT−Per3 ([SWCNT] = 0.057 g/L, $[Per3]_i$ = 0.1 wt%); the total amount of SDBS added corresponds to a SDBS concentration of 0.03 wt%: (a) λ_{exc} = 660 nm and (b) λ_{exc} = 785 nm.

SDBS. They observed fluorescence quenching due to rebundling of the nanotubes upon dilution of the surfactant at a SDBS concentration of 0.023 wt% which is also well below the critical micelle concentration. Although we observe debundling of nanotubes at a much lower SDBS concentration (0.01 wt%), this is not in marked contrast to the observations of McDonald et al. It has to be considered that we determined the minimum concentration of SDBS necessary to successfully debundle any SWCNTs, while McDonald et al. were interested in the concentration of SDBS at which rebundling starts to occur when a widely debundled sample is diluted. Upon stepwise addition of a solution of SDBS to nanotubes dispersed by Per3, striking differences in the fluorescence spectra are observed when the concentration of SDBS in the solution exceeds 0.026 wt%: the fluorescence intensity is strongly increased and the structural pattern is changed. Obviously, replacement of the perylene adsorbed on the sidewall of the nanotubes takes place (as revealed by Raman and UV/vis/nIR absorption spectroscopy) when the concentration has reached 0.026 wt%, resulting in an increase of fluorescence intensity and regeneration of the spectral pattern of SWCNTs dispersed in an aqueous solution of SDBS. However, in the presence of Per3, a much higher concentration of SDBS is needed to create nIR emission spectra similar to spectra of pristine SWCNTs in an aqueous solution of SDBS than is necessary to individualize SWCNTs in the blank experiment. We suspect that, in the presence of Per3 adsorbed on the nanotube, a higher concentration of SDBS has to be exceeded for replacing the perylene from the nanotube sidewall, as the negatively charged perylene molecules shield the nanotubes from the adsorption of SDBS. As soon as these electrostatic forces are overcome at a certain concentration of SDBS, SDBS molecules replace the perylene, thereby reducing the electrostatic repulsion, allowing more SDBS molecules to adsorb on the nanotubes, resulting in a sudden change (pattern and intensity) of the fluorescence spectrum.

Since Per3 is an amphiphilic molecule, the formation of mixed micelles of SDBS and Per3 may also account for this sudden change. Per3 is theoretically capable of binding to the nanotube surface via two different mechanisms:[42] on the one hand, the polyaromatic perylene core may bind to the nanotube surface via $\pi-\pi$-stacking interaction and on the other hand SWCNTs may be enclosed in the micelles of the amphiphilic perylene derivative **3**. We have found strong evidence for a $\pi-\pi$ interaction between the perylene unit and the SWCNT in optical absorption and emission spectroscopy which favors dispersion via the first mechanism. However, upon addition of SDBS to a dispersion of SWCNTs in an aqueous solution of Per3, the binding mechanism may change by the formation of mixed perylene−SDBS micelles. The formation of micelles consisting of Per3 and SDBS presumeably results in an increase of the fluorescence intensity of Per3, as self-aggregation of the perylene moieties is reduced hereby. When mapping the addition of an aqueous solution of SDBS to a buffered, aqueous solution of Per3 by the fluorescence of the perylene (with an excitation wavelength of 500 nm), the emission intensity was found to increase with increasing concentration of SDBS. This result suggests that SDBS is indeed inserted in the perylene micelles within the concentrations range studied ([Per] = 0.1 wt%, final concentration of SDBS = 0.03 wt%) here.

Furthermore, even though the drastical and rapid change of the fluorescence spectrum of SWCNT−Per3 upon addition of a solution of SDBS can be explained, it remains unclear why merely the fluorescence of specific (*n*,*m*)-SWCNTs is quenched completely in a buffered aqueous solution of nanotubes in Per3, while being partly preserved for others. Possibly, selective individualization of certain SWCNTs species is responsible for this observation. Further investigations concerning selectivity and electronic or energetic communication between the perylene molecules and the nanotubes will supposedly shed light on the highly interesting emission behavior of nanotubes dispersed by the investigated perylene.

Conclusion

We have demonstrated that SWCNTs can be very efficiently dispersed with a pronounced degree of individualization in buffered aqueous media by a water-soluble perylene bisimide derivative even at perylene concentrations as low as 0.01 wt% as shown by UV/vis/nIR absorption spectroscopy. The characteristic nanotube features (vHS) appear red-shifted in SWCNT−Per3 compared to SWCNTs dispersed in an aqueous solution of SDBS strongly supporting $\pi-\pi$-stacking interaction. This is further evidenced by a red-shift of the $\pi-\pi^*$ and $n-\pi^*$ transitions of the perylene unit in SWCNT−Per3 relative to an aqueous solution of Per3 without nanotubes. From the presence of signals in nIR emission spectroscopy, it can be concluded that individualization of the pristine nanotube material has occurred. Significantly, the fluorescence signals are reduced in number and appear red-shifted for smaller diameter nanotubes and blue-shifted for larger diameter nanotubes in SWCNT−Per3 compared to spectra taken in a solution of SDBS because of the changed chemical surrounding. This together with the observed quenching of the perylene fluorescence caused by

the $\pi-\pi$ stacking interaction with the sidewalls of the tubes demonstrates that the adsorption of the perylenes is accompanied by pronounced electronic communication, such as photoinduced energy or electron transfer.[43−45] For the first time such an interaction of SWNCTs has been demonstrated with an electron poor aromatic system serving as an acceptor. The presence of individual SWCNTs has been underscored by AFM and cryo-TEM investigations revealing a high population of individual SWCNTs. It has been shown by Raman spectroscopy that the perylene units are replaced by SDBS upon addition of an aqueous solution of SDBS to the nanotubes dispersed in a buffered aqueous solution of Per3. As fluorescence spectroscopy reveals, a certain threshold of SDBS concentration has to be exceeded. To elucidate the nature of the perylene adsorption in more detail, further investigations involving time-resolved optical spectroscopy will be carried out in order to quantify this interesting electronic communication of SWNTs, which is described here for the first time. Such studies will be of importance for the further integration of SWNTs as components for electronic devices. Another topic of interest is certainly the investigation of whether or not individualization occurs selectively. A fine discrimination in the diameters of SWCNTs upon solubilization combined with the recent progresses concerning separation of solubilized carbon nanotubes by density gradient ultracentrifugation is expected to give access to a larger amount of specific (*n*,*m*)-SWCNTs.

Acknowledgment. We thank the Deutsche Forschungsgemeinschaft (DFG) and the Interdisciplinary Center for Molecular Materials (ICMM) for financial support. We also thank Ralf Graupner for numerous fruitful discussions.

Supporting Information Available: Optical absorption and emission spectra of the addition of Per3 to SWCNTs in buffered water, excitation−emission contour plots of SWCNT−Per3 and SWCNT−SDBS, solution Raman spectra of SWCNT−Per3, and fluorescence spectra of SWCNT−SDBS dispersions. This information is available free of charge via the Internet at http://pubs.acs.org.

JA805660B